Microfiber Hotspots Association with Ships in a Remote Port Before and During Covid-19

Guyu Peng [a,b,*], Caroline Mengeot [c], Chunhua Jiang [b], Baile Xu [d], Xin Zhong [e], You Song [f], Feng Zhang [b], Daoji Li [b,*]

a The Key Laboratory of Water and Sediment Sciences, Ministry of Education, College of Environmental Sciences and Engineering, Peking University, Beijing, 100871, P. R. China.

b State Key Laboratory of Estuarine and Coastal Research, East China Normal University, 500 Dongchuan Road, Shanghai, 200241, P.R. China

c Norwegian Institute for Water Research (NIVA), Thormølensgate 53D, N-5006 Bergen, Norway

d Institute of Biology, Freie Universität Berlin, Altensteinstr. 6, D-14195 Berlin, Germany

e Institute of Geological Sciences, Freie Universität Berlin, D-12249 Berlin, Germany

f Norwegian Institute for Water Research (NIVA), Økernveien 94, Oslo N-0579, Norway

Corresponding Authors

*Guyu Peng, The Key Laboratory of Water and Sediment Sciences, Ministry of Education, College of Environmental Sciences and Engineering, Peking University, Beijing, 100871, P. R. China. E-mail: guyu.peng@pku.edu.cn

*Daoji Li, State Key Laboratory of Estuarine and Coastal Research, East China Normal University, 500 Dongchuan Road, Shanghai, 20024, P.R. China. E-mail: daojili@sklec.ecnu.edu.cn

ABSTRACT

During monthly water quality monitoring of Norwegian coastal waters, sea surface waters off Brønnøysund, a remote port of Norway, exhibited unexpected high abundance of microfibers. We further conducted monitoring of microplastics and microfibers from surface waters off the city before and during the Covid-19 pandemic. Analysis of the microfiber characteristics, which were primarily comprised of cellulosic and polyester fibers, revealed similarities with those found in the global ocean, but at concentrations that were 1-4 orders of magnitude higher, with the maximum concentration reaching 491 n/L (0.34 mg/L). Source apportionment of microfibers using multivariate analyses based on simultaneous water chemistry data showed positive correlations with ships. Contrary to previous assumptions that marine microfibers were derived from land-based sources, our findings revealed that gray water discharge from ships significantly contributed to microfibers in the oceans. The demonstrated causations using path modelling between microfibers, gray water, shipping and non-cargo shipping activities call for urgent research and regulatory actions towards addressing plastic pollution in the UN Decade of Ocean Science.

SYNOPSIS

Sea-based sources of microplastics and microfibers have been considered minor. This study discovered a pollution hotspot with high concentrations of microfibers in a remote area and its association with gray water discharge from ships.

KEYWORDS

Microfibers, Microplastics, Shipping, Norway, Marine pollution, Gray water

TOC

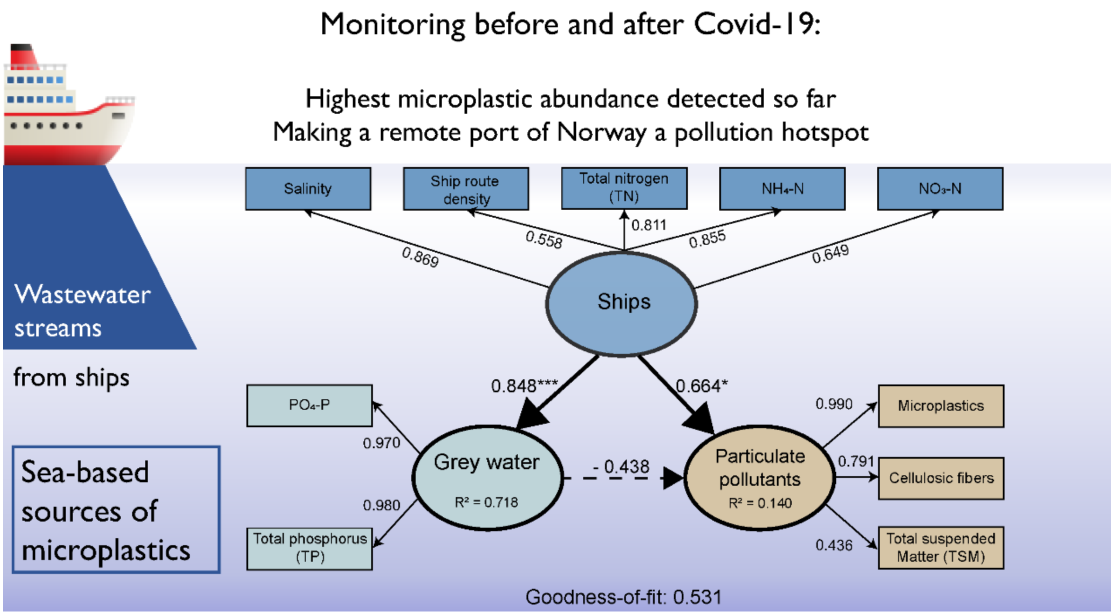

Monitoring before and after Covid-19:
Highest microplastic abundance detected so far
Making a remote port of Norway a pollution hotspot
Wastewater streams
from ships
Sea-based sources of microplastics
Salinity
Ship route density
Total nitrogen (TN)
NH_4-N
NO_3-N
0.869
0.558
0.811
0.855
0.649
Ships
0.848***
0.664*
PO_4-P
0.970
0.980
Total phosphorus (TP)
Grey water
R^2 = 0.718
- 0.438
Particulate pollutants
R^2 = 0.140
0.990
0.791
0.436
Microplastics
Cellulosic fibers
Total suspended Matter (TSM)
Goodness-of-fit: 0.531

Introduction

Plastics debris and microplastics as emerging marine environmental pollutants have gained increasing attention worldwide. The United Nations Environment Assembly (UNEA) addressed urgent need of research and information on the identification of pollution sources since UNEA-1 [1]. Microparticles (MP) including microplastic and microfibers contain diverse members in the polymer universe, with increasing reports on the presence of natural cellulosic fibers in the global ocean [2]. Sea-based sources of plastic waste include maritime activities, aquaculture and fisheries [3], and regulatory practice in shipping activities has focused on solid waste management (i.e., MARPOL Annex V, www.imo.org). Nonetheless, quantitative understanding on how land- and sea-based sources contribute to MP in the ocean are lacking, thus impeding precise regulation and innovation [4]. Wastewater treatment plants are regarded as major land-based sources of microplastics and microfibers in the aquatic environment [5], but empirical data on MP in waste streams at sea from ships are lacking [6]. Important sources of pollutant discharge, such as black water and gray water from ships have just begun to be recognized [7]. While black water is also known as sewage water, gray water refers to waste streams from baths, galleys, laundry, washbasins and sinks [8], and is considered a significant sea-based source~~s~~ of MP input to the ocean [6]. Identification of MP inventory is thus critical for preventing plastic accumulation in the ocean [9].

Aquaculture and fisheries are also contributors to MP pollution in coastal areas [10]. Many studies have documented the presence of MP in aquaculture species [11]. Cultured species are exposed to higher risk of MP ingestion once released from plastic aquaculture systems [12], and the exposure of organisms are dependent on feeding strategies and environmental concentration of MP [13]. Moreover, micro(nano)plastics and microfibers are of possible human health concern through inhalation of MP particles and ingestion of contaminated food and water [14]. A project to monitor water quality in Norwegian coastal waters was conducted in the period of 2014-2020 [15]. One of the sampling sites, Brønnøysund, is a 3.38 km^2 coastal city with a population of 5,045 (2018) and is a port city that is frequently visited by cruise ship passengers. It is also a typical aquaculture area in Norway where the Norwegian Aquaculture Centre is located (Figure S1, Table S1). During routine sampling in Brønnøysund for water quality of coastal surface waters, high quantities of micro-sized fibers were often encountered, and an in-depth investigation on MP pollution, especially microfibers and its source apportionment, followed.

Here, we investigated temporal variation and vertical distribution of MP in a remote port of Norway before and during Covid-19. We systematically characterized the morphology and polymer type of the MP samples, and traced their possible sources by analyzing their relationships with water chemistry and hydrology. Our results showed a positive correlation between MP and ships, particularly gray water discharge from ships. To establish causality between MP pollution, ships and gray water, we employed a structural equation model. Additionally, we discussed the impact of Covid-19 pandemic on MP pollution in the ocean. This study aims to provide the important evidence highlighting sea-based sources, as opposed to land-based sources, of MP pollution in the marine environment.

Materials and methods

Sampling, identification and quantification of MP

The sampling site at Brønnøysund (65.6009N, 12.2354E) was named VR31 and is located in the Tilremsfjord area, with water depth of ca. 260 m, 14 km away from the city (Figure S1). Eight sampling for MP were conducted from September 2019 to March 2021 alongside a water quality monitoring program along the Norwegian coasts by Norwegian Institute for Water Research (NIVA) and Statens naturoppsyn (Norwegian Nature Supervision Authority, SNO) with the exception of Covid-19 outbreak periods. Simultaneous water chemistry parameters were derived from published reports [15]. Before each sampling, five pieces of 63-μm nylon meshes were cut into ca. 20 cm × 20 cm squares and wrapped in aluminium foil. Water samples were taken at depths of 0 m, 5 m, 10 m, 20 m and 30 m with a 6-L Niskin bottle. The collected water was filtered a short time after the sampling on shore with a portable filtration device designed for this study (Figure S2). Prior to sampling, bottles and meshes were rinsed with seawater. At each depth, 1 L of water was filtered through 63-μm nylon mesh connected to the portable water filtration device. Details of sampling site and sampling method see Text S2-3, Supporting Information. The outer garments from the technician during sampling were listed in Table S3, which were all made of synthetic materials and did not contribute to the cellulosic microfibers in the results.

In the lab, sample treatment and identification followed recommended protocols in a worldwide inter-laboratory study [16] . Visual inspection by microscopy (Leica M165 FC, Germany and OPTEC, TP510, China) and chemical identification (Thermo Fisher Nicolet iN10 and Perkin Elmer Spotlight 200) was performed. Detailed instrumental setting see Text S3. QA/QC is performed throughout sampling and lab analysis, for details see Text S4. No contamination of airborne fibers was found for procedural blanks by adding Milli Q water during filtration. Based on scoring criteria for microplastic analysis [17], the assessment results on data quality of this study was among the highest reliability for surface water sampling (Table S2).

The direct reporting unit from identification process was number concentration (n L^{-}

[1]). To better compare with other water quality parameters, number concentration was converted into mass concentration with the following equation. Assuming cylindrical shape of fibers, the mass of MP at each site (CM) is calculated using Eq. 1:

$$CM = \frac{\sum_{i=1}^{n} \pi r^2 h_i \times \rho}{k} \quad (1)$$

where r is the radius of the fiber of 10 μm [18, 19], h is the length of a fiber, k is the sampling volume of 1 L at each depth, ρ is the density of polymer, and we assumed 1.5 g cm^{-3} for MP fibers.

Statistical analysis

Normality and equal variance were checked prior to statistical analysis. The significance level α was set at 0.05, and all the tests were two-tailed. Two sample t-test was applied for difference in MP concentration before and during Covid-19 and for water chemistry parameters between high and low MP groups. Non-parametric Kruskal Wallis test in combination with Dunn' test was performed to compare MP abundance and size distribution of MP. Wilcoxon signed rank test was performed to understand if MP abundance differed before and during Covid-19 or between high and low MP groups. Spearman's correlation was used to calculate relationships between MP abundance and other water chemistry parameters. Principal component analysis (PCA) was applied to understand the factors that influenced water quality of each sampling dates. All statistical and graphical work was conducted using OriginPro 2020b (OriginLab Corp., Northampton, USA) or Graphpad Prism 9.0.0 (San Diego, USA).

Partial Least Squares Path Modelling (PLS-PM)

The Partial Least Squares Path Modelling (PLS-PM) was applied to explore the causal relationship between shipping and non-cargo shipping activities, nutrients and

MP concentrations. PLS-PM is a multivariable method and a Partial Least Square approach to Structural Equation Modelling (SEM) considering a dataset < 200 observations [20]. The model statement for relationships between latent variables is that ships contributed to gray water and particulate pollutants. Each block in the framework with observations plays a role of a latent variable. Linear relationships were assumed for each edge (relationship between two blocks), making the framework a system of multiple interconnected linear regressions. PLS-PM was performed using the package "plspm" in R [20].

Results

Temporal and vertical distribution of MP in surface and sub-surface water

A total of 1428 MPs were detected before Covid-19. During MP monitoring from September 2019 to January 2020 (Figure 1), the average MP abundance of four samplings before Covid-19 was 71.0±53.9 (mean±SD) n L^{-1} by number, and 0.024±0.019 mg L^{-1} by mass. The highest MP abundance in surface and sub-surface water at Brønnøysund reached 200 n L^{-1} at 0 m in Sept. 2019, and the lowest concentration was at 10 m in Nov. 2019 at 16 n L^{-1}. The mean abundance for Sept. 2019, Nov. 2019, Dec. 2019 and Jan. 2020 was 140.4±55.0, 34.6±23.3, 37.0±9.1 and 73.6±29.3 n L^{-1}, respectively. MP and chlorophyll-a concentration, and colour composition at each depth from 0-30 m during the sampling period before Covid-19 is visualized in Figure 1a-h. Major colour categories included blue (32.8%), black (20.6%), red (25.8%) and transparent (10.1%). Fibers constituted 97.8%, and fragments constituted 1.5% of the total MP, followed by film (0.4%) and sphere (0.2%) of all the suspected particles. As most fishing nets are stained in green, fibers from the present study were not derived from fishing nets. Green particles consisted 0.6% of total MP, and were thus included in the “other” category. **The absence of spheres made from extended polystyrene (EPS) foam for buoys and few green polyamide or polyethylene fibers for fishing nets excluded aquaculture and fisheries as major sources of MP in the hotspot**.

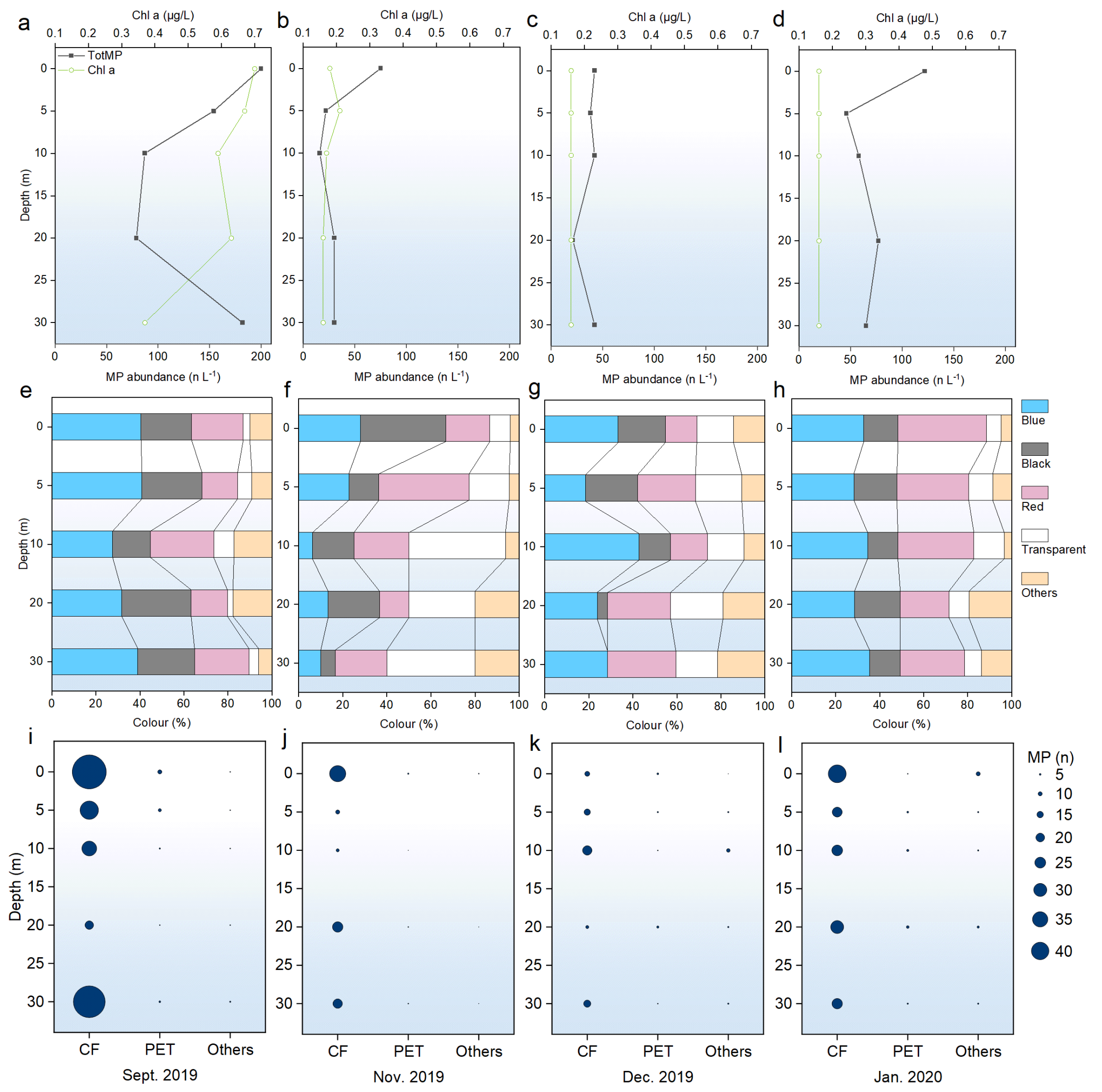

Figure 1. Characteristics of microplastics and microfibers during coastal surface water monitoring (0 – 30 m) in Brønnøysund, Norway before Covid-19. (a-d) MP abundance, chlorophyll-a concentration at each depth, (e-h) colours of MP at each depth, and (i-l) polymer composition at each depth. CF: cellulosic fibers, PET: polyethylene terephthalate, Others: all other

polymers detected.

A total of 12 polymers were identified via μ-FTIR analysis (n = 668). The majority of identified polymers were cellulosic fibers (81.3%) and polyethylene terephthalate (PET) (10.3%). Other polymer types included polypropylene (PP, 2.84%), polyamide (PA, 1.2%), polyethylene (PE, 1.2%), polyacrylonitrile (PAN, 1.1%), polyacrylic acid (PAA), polyvinyl chloride (PVC), olefin, polystyrene (PS) and polyether. The density of these polymers varied from 0.88 g cm^{-3} (PP) to 1.7 g cm^{-3} (PVC).

The average abundance of MP at 0 m, 5 m, 10 m, 20 m, 30 m during the sampling period before Covid-19 was 109.8±68.5, 65.0±60.2, 50.8±29.7, 51.8±30.5 and 79.8±69.7 n L^{-1}, respectively. No significant difference between MP abundance among depth groups was found (Kruskal Wallis ANOVA test, df = 4, p = 0.63). The vertical distribution of polymers from 0-30 m is shown in Figure 1i-l. The mean and median size of MP at 0 m, 5 m, 10 m, 20 m and 30 m exhibited an increasing size at deeper layers (Figure S3). Size distribution of MP by length at 0 m was different from 20 m (Kruskal Wallis ANOVA test, df = 4, p = 0.0097) and 30 m (p = 1.53E-4). Surface water at 0 m retained most MP, but an increased concentration at 30 m layer can be explained by the influence of seasonal thermocline/halocline [21] or other pollution sources.

A total of 1583 MP were detected in water samples during Covid-19, with 99.37% being fibers. The average MP abundance during Covid-19 was 79.1±103.1 n L^{-1} by number, and 0.044±0.070 mg L^{-1} by mass (Figure S4, Figure 2d). The maximum concentration was 491 n L^{-1} at 30 m, Jan. 2021, and the minimum concentration was 18 n L^{-1} at 30 m, Sept. 2020. The mean abundance for Sept. 2020, Oct. 2020, Jan. 2021 and Mar. 2021 was 27.0±5.8, 45.4±6.6, 186.4±173.6 and 57.8±22.0 n L^{-1}, respectively.

Size distribution of MP among depth layers were highly different (Kruskal-Wallis ANOVA, df = 4, p = 1.3E-10, Figure S3), and size distribution at 30 m was different from all the other layers ($p < 0.01$). This is similar to the results before Covid-19 that size distribution of MP at deeper layers were different from the surface, which can be attributed to the formation of halocline that entraps MP [21, 22]. The mean and median size also increased as depth increased, but the larger size during Covid-19 compared to that before Covid-19 can be attributed to the difference in the resolutions of stereomicroscopes. Eight polymer types were identified for MP samples during Covid-19 (n = 599), including cellulosic fibers (86.8%), PET (7%), PAN (3.17%), PP (1.5%), PS (0.5%) PA (0.2%) and one alkyd paint particle. Fibers constituted 99.37% of MPs in addition to fragments and films. Blue (50.5%), black (24.6%), red (10.6%) and transparent (8.5%) MPs are the prevalent colours, which shared similar MP characteristics with that before Covid-19.

Comparison of MP abundance before and during Covid-19

Characteristics and polymer composition of MP in the present study resembled that from a global investigation of MP in oceanic surface water, indicating comparable results for interpretation of MP concentration with similar analytical methodology and reporting units [2]. Similarly, cellulosic fibers constituted the majority of MP throughout the global investigation, and MP size were at similar size ranges [2]. However, global MP concentrations were one to four orders of magnitude lower (0.02-25.8 n L^{-1}) compared to that from the present study (16-491 n L^{-1}), indicating that the sampling site is a hotspot of MP pollution in the world's ocean, which is unique for a remote place like Brønnøysund with very good water quality based on monitoring results of 2014-2019

[15].

Depth profile of MP concentration before and during Covid-19 is shown in Figure 2. MP abundance of each month exhibited large variability during the entire sampling period from 2019-2021 (non-parametric Kruskal Wallis ANOVA test and Dunn's multiple comparison test, df = 7, p = 9.93E-5). MP concentration in Sept. 2019 and Jan. 2021 differed significantly from Sept. 2020 (p = 0.004 and p = 0.009, respectively), indicating a distinction between sampling dates with high and low MP concentrations (Figure 2a). Therefore, in order to understand the sources of MP, we regrouped the dataset by high MP dates (Sept. 2019, Jan. 2020, Jan. 2021 and Mar. 2021), and low MP dates (Nov. 2019, Dec. 2019, Sept. 2020 and Oct. 2020). MP concentration **before and during Covid-19** did not exhibit difference by number (Wilcoxon signed rank test, p = 0.72) or by mass (p = 0.40, Figure 2c-d), but differed significantly for **high and low MP dates** by number (Wilcoxon signed rank test, p = 2.19E-4) and by mass (p = 0.0011, Figure 2c-d). **High MP concentration behind excellent water quality led to further analysis on potential MP sources based on simultaneously collected water chemistry parameters. Therefore, in the following sections, we categorized MP and water chemistry data into "high MP dates" and "low MP dates" instead of "before Covid-19" and "during Covid-19".**

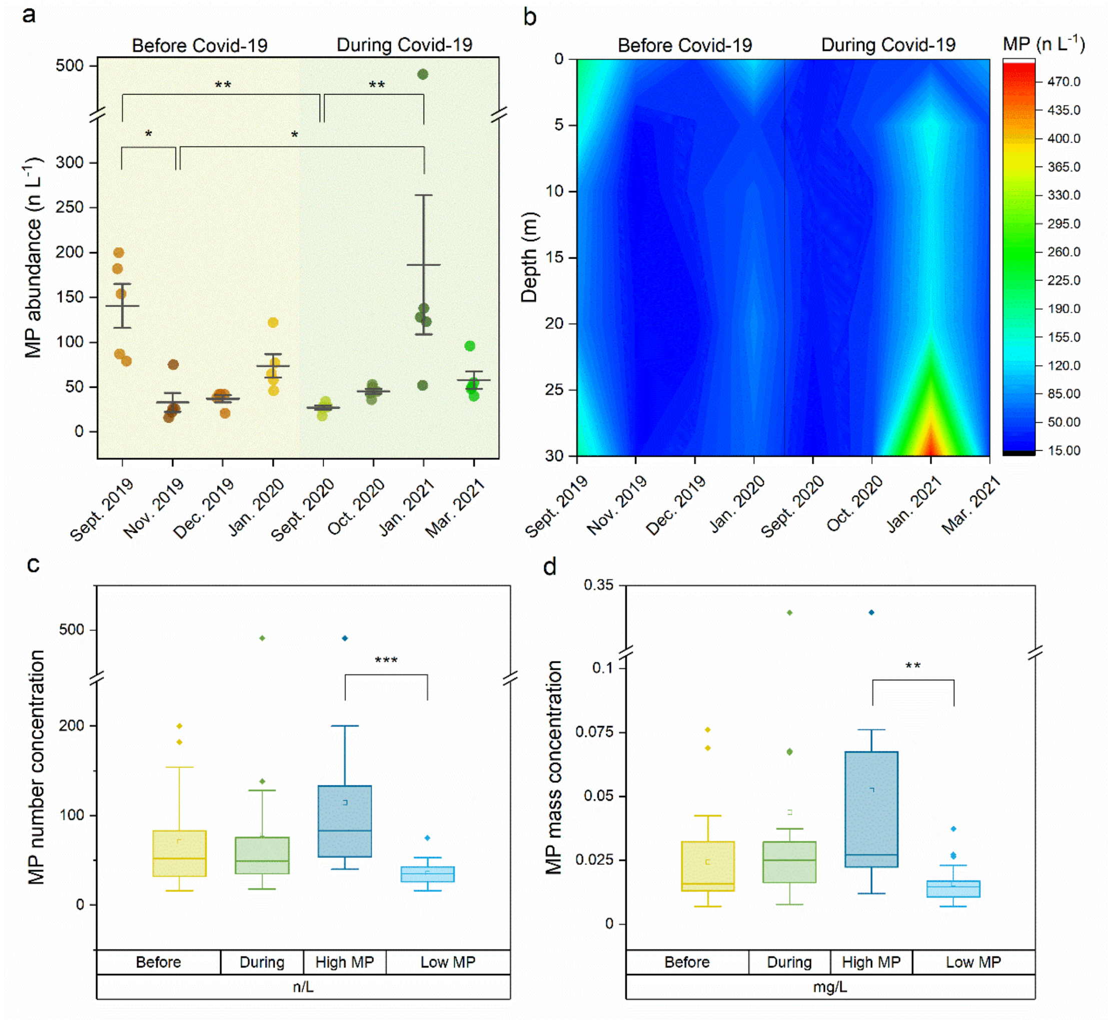

Figure 2. MP abundance by number and by mass in surface and sub-surface water (0 – 30 m) in Brønnøysund, Norway before and during Covid-19. (a) MP abundance for each month (mean ± SE) and (b) MP on the depth profile during the sampling period from 2019–2021. High MP dates were significantly different from low MP dates (non-parametric Kruskal Wallis ANOVA test and Dunn's multiple comparison test, df = 7, $p < 0.001$). (c) Number concentration and (d) mass concentration of MP before and during Covid-19 on high MP dates and low MP dates, respectively. MP abundance did not differ significantly before and during Covid-19 by number (Wilcoxon signed rank test, $p > 0.05$) or by mass ($p > 0.05$), but high MP dates differed significantly from low MP dates by number ($p < 0.01$) and by mass ($p < 0.01$). The upper and lower box extends from the 25th to 75th percentile, and the whiskers extend from minimum to maximum excluding outliers (* < 0.05, ** < 0.01, *** < 0.001).

MP associated water chemistry and hydrography

According to the five-year monitoring results from 2014-2019 [15], water quality in Brønnøysund at the station VR31 was "very good" for phytoplankton and "good" to "very good" for supportive elements (e.g., nutrients, total suspended matter). The sub-program in 2019 and 2020 also classified water quality in Brønnøysund as "good" for decisive parameters (total phosphorus, TP) to "excellent" for other supportive elements. Stratification of surface water prevents mixing of surface water and deep water, thus entrapping dissolved and suspended matter in the surface water. Monitoring results of temperature, salinity of the sampling station VR31 from 2014-2020 indicated a stratification layer at around 50-100 m starting from summer to the end of the year [15]. Regarding the elevated level of TP, a major anthropogenic source of phosphorus is cleaning detergents in waste streams at sea, especially gray water that receives laundry water [6].

Although the station VR31 at Brønnøysund has good vertical mixing and very good water quality, orthophosphate (PO_4-P) and total phosphorus (TP) were the highest compared to other monitoring sites in southern Norway [15]. Correlation between MP concentration and other water chemistry parameters before and during Covid-19 was calculated (Figure S5). Positive correlations were found between MP and ammonia nitrogen (NH_4-N) before and during Covid-19 (Spearman r = 0.56, p = 0.01 and r = 0.71, p = 0.001, respectively). Ammonia is indicative of human waste in wastewater from ships that usually exceeds urban wastewater discharge criteria, although dispersion in the sea is fast after discharge [8]. **These monitoring data on N, P led to our analyses on MP associated N, P and other water chemistry parameters before and during Covid-19** (Figure 3).

Source apportionment of MP based on water chemistry

We further analysed water chemistry parameters during high MP dates in Sept. 2019, Jan. 2020, Jan. 2021 and Mar. 2021 before and during Covid-19 (Figure 3a-c). Although nitrogen and phosphorus may include both natural and anthropogenic sources, as initial guess for anthropogenic sources, we found that high MP dates exhibited higher nutrition contents (TN, TP) and higher total suspended matter (TSM) compared to low MP dates, with TP significantly differed between high and low MP groups (two sample t-test, $t = 2.487$, $df = 38$, $p = 0.018$). MP as particulate pollutants may disperse much slower and remain buoyant at sea surface compared to the dilution of N and P after discharge, which led to low correlation with MP in general (Figure S5) but higher N and P concentration on high MP dates.

Principal component analysis (PCA) further revealed the relationship between MP and other water chemistry parameters on each sampling date (Figure 3d-e). Nutrients (N, P) has high loadings on PC1, and PC2 was directly explained by total MP, cellulosic MP and TSM. That is, MP and TSM shared similar composition, and MP became the dominant type of TSM on high MP dates. It is a surprising finding, because MP as anthropogenic pollutants has exceeded sediment, silt, clay, plankton, algae or other natural matter to dominate TSM. Based on PCA results, high MP dates on Jan. 2021 and Mar. 2021 showed high scores on PC1 and PC2, indicating simultaneous presence of high nutrients and high MP.

This is further evidenced by a microscopic photo of the filter membrane with the highest MP concentration from 30 m Jan. 2021, which shows that hundreds of MP were retained on the filter after directly filtering 1 L seawater, far exceeding natural matter (Figure 4b). High MP date on Jan. 2021 exhibited highest scores on PC2, and TSM concentration from 30 m Jan. 2021 was also the highest (0.53 mg L^{-1}) among all the water samples. The respective MP mass concentration reached 0.34 mg L^{-1} based on our mass calculation, which indicated that 64% of TSM is comprised of MP. The ratio of MP/TSM in the water column was also the highest for Jan. 2021 (31±17%) across all layers compared to all other dates (1.9%-17.2%).

Specifically, in the monitoring program along Norwegian coasts from 2017-2019, Visibility of the sampling site VR31 averaged 9.84 m during 2014-2019, indicating very low turbidity. However, the highest TSM concentration reached 2 mg L^{-1} at 5 m on Oct. 2018, while all the other TSM concentration during 2017-2019 did not exceed 1 mg L^{-1} [15]. Such high TSM concentration at one specific depth could only attribute to pollution events, e.g., discharge of waste streams from ships at 5 m below the ship's waterline [8].

The *Redfield ratio* determines proportions of principal elements absorbed by aquatic plants from seawater as C:N:P = 106:16:1 for algal production [23]. Generally, N is the limiting nutrient for phytoplankton when N:P is lower than 16:1, whereas P being the limiting nutrient when N:P is higher than 16:1 in the open ocean [24]. TN and TP showed N limiting for primary production in the study area in coastal wasters (Figure 3f-g) in that all data points were situated on the right side of the reference line of the *Redfield ratio*, showing very good mixing of water masses in the study area. Low MP dates exhibited N limiting, while high MP dates exhibited a trend towards P limiting, indicating excess N discharge during high MP dates.

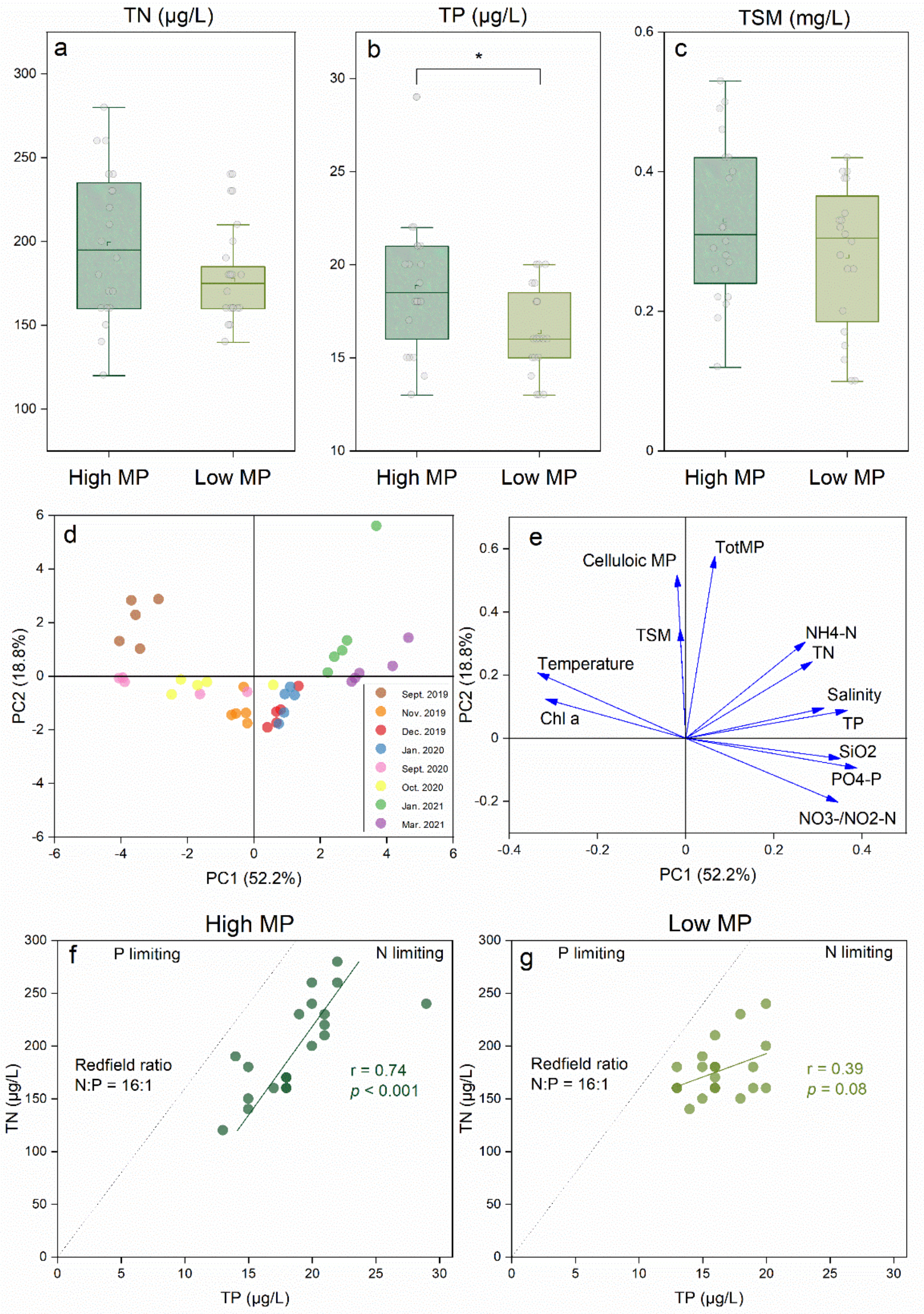

Figure 3. Water chemistry parameters indicating MP associated N, P discharge and its influence on total suspended matter (TSM). (a) Total nitrogen (TN), (b) total phosphorus (TP) and (c) TSM observed during high MP dates and low MP dates. TN, TP and TSM are higher for high MP dates compared to low MP dates. The horizontal lines and squares show the median and mean. The upper and lower box extends from the 25th to 75th percentile, and the whiskers extend from minimum to maximum excluding outliers. (d-e) The score plot and loading plot of the principal

component analysis (PCA) of water chemistry parameters for eight sampling dates. PCA results showed that N, P had high loadings on PC1, and PC2 is explained by cellulosic particles, which also contributed to TSM. (e-f) The ratio of N:P for (e) high MP dates and (f) low MP dates compared to the *Redfield ratio*, indicating N limiting for primary production in the study area, and high MP dates showed excess N input with the rising slope towards the *Redfield ratio*.

MP associated water chemistry revealed that the source of high MP pollution was related to simultaneous N, P discharge, increased TSM and higher primary production. Considering that MP in wastewater from WWTPs is also dominated by fibers [25], wastewater streams is the medium that meets all the characteristics in terms of water chemistry and MP composition. **Extensive shipping and non-cargo shipping activities in the study area that discharge waste streams along travel routes were making the study area MP hotspots, considering the proximity of the sampling site to the most densely traveled ship routes near the port city of Brønnøysund** (Figure 4a) **by comparing the monitoring results from 2019-2021 to all other reports from surface seawater worldwide** (Figure 4d).

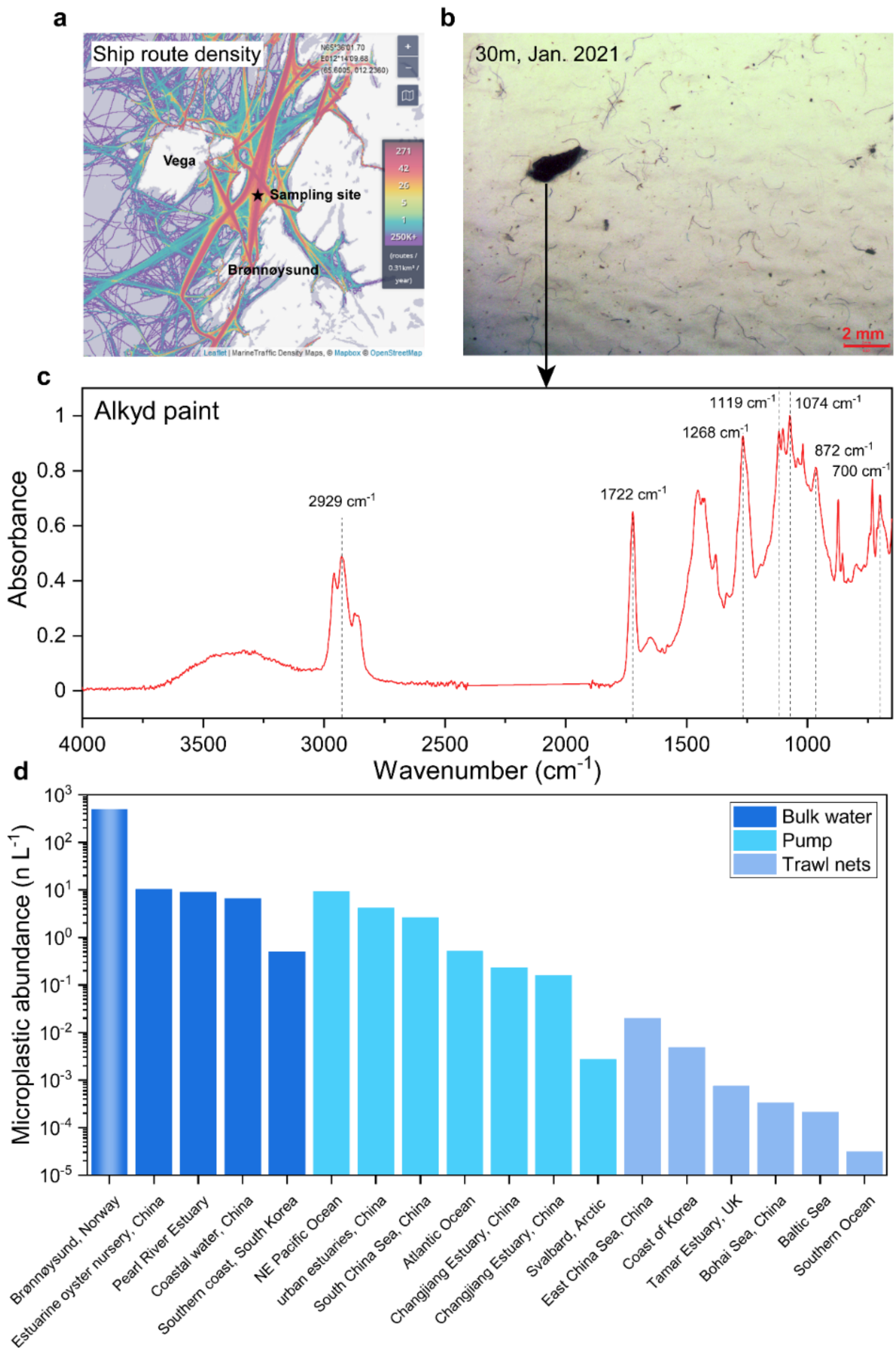

Figure 4. The microfiber hotspot association with shipping and non-cargo shipping activities, making the study area a hotspot of microfiber pollution in the global ocean. (a) Ship route density of the study area in 2020 (data from marinetraffic.com). (b) Microscopic photo of MP on the filter from 30 m Jan. 2021 with the highest abundance at 491 n L^{-1} and (c) a particle identified as alkyd ship paint from that depth layer. The scale bar represents 2 mm. (d) MP abundance in

Brønnøysund, Norway was the highest compared to surface water concentration worldwide.

Microfiber hotspots association with shipping and non-cargo shipping activities

MP variation during the study period exhibited similar trend as the ship route density data (routes km^{-2} month^{-1}, data from EMODnet) at the sampling site (linear fit, $r = 0.64$, $p < 0.05$, Figure 5a-b). Compared to reports from surface seawater worldwide [26-42], MP abundance before and during Covid-19 in the waters off the remote port city of Norway was the highest (Figure 4d). By comparing the coordinates of the sampling site to the ship route density map, VR31 was situated on the busiest shipping route of the study area in 2020 (Figure 4a, map from Marinetraffic.com, last accessed 20/09/2021), which confirmed unneglectable pollution from ships even during Covid-19 (Figure S6). Meanwhile, positive correlations were observed between ship route density-TP ($p < 0.05$, Figure S7a), ship route density-TN ($p < 0.05$, Figure S7b), and MP-TP ($p < 0.05$, Figure S7c). Shipping and non-cargo shipping activities as a major source of MP is further corroborated by the lowest concentrations during Sept.-Oct. 2020. This period was when all the cruise ships travelling along Norwegian coasts were restricted due to Covid-19 (Figure S6). Since Jan. 2021, cruise ships started to increase frequency and operated in full capacity until June 2021, while other types of ships remained in operation even during the Covid-19 (Figure S6).

Among 3011 particles detected before and during Covid-19, an alkyd paint from 30 m depth on Jan. 2021 was identified using ATR-FTIR due to its opaque texture and larger particle size (Figure 4b-c). Alkyd paint is a common polymer in marine paints due to its good permeability and long durability for anticorrosive purposes, often made of polyester, polyols and organic acids [43, 44]. After initial library search indicating alkyd and polyester composition, the paint particle was confirmed with absorption bands at

2929, 1722, 1268, 1119, 1074, 872 and 700 cm^{-1}. The band at 2929 cm^{-1} indicated C-H stretching vibrations [44]. The strong band at 1722 cm^{-1} indicated saturated C=O stretching vibration. The bands at 1268, 1119 and 1074 cm^{-1} indicated the presence of C-O-C. The band at 872 cm^{-1} indicated C-O out of plane bending. The band at 700 cm^{-1} confirmed a monosubstituted benzene ring [45]. Interestingly, the depth where the paint particle was present had the highest MP concentration (30 m Jan. 2020), reaching 491 n L^{-1} MP (Figure 4b-c).

To confirm the causal relationship among all the variables including MP, ships and nutrients, we applied the Partial Least Squares Path Modelling (PLS-PM) [20]. Cause-effect relationships were established between three latent variables (LVs) in the inner model, and ten manifest variables (MVs) in the outer model (Figure 5c). Density of ships is indicated by ship route density and sewage from ships (NH_4-N, TN, NO_3-N). Even ships equipped with WWTPs, sewage discharged from ships exceeds domestic wastewater standards [8]. Sewage is discharged quickly after generation due to limited wastewater capacity of ships, linking the amount of sewage discharge to the ship density [6]. Our finding proved that MP comprised 64% of TSM at high concentrations, indicating that TSM under the influence of MP should be regarded as an indicator for particulate pollutants. After adjusting the model repeatedly, the Goodness-of-fit (GoF) of the model yielded 0.531, indicating good prediction results. Detailed results of the PLS-PM model see Text S5.

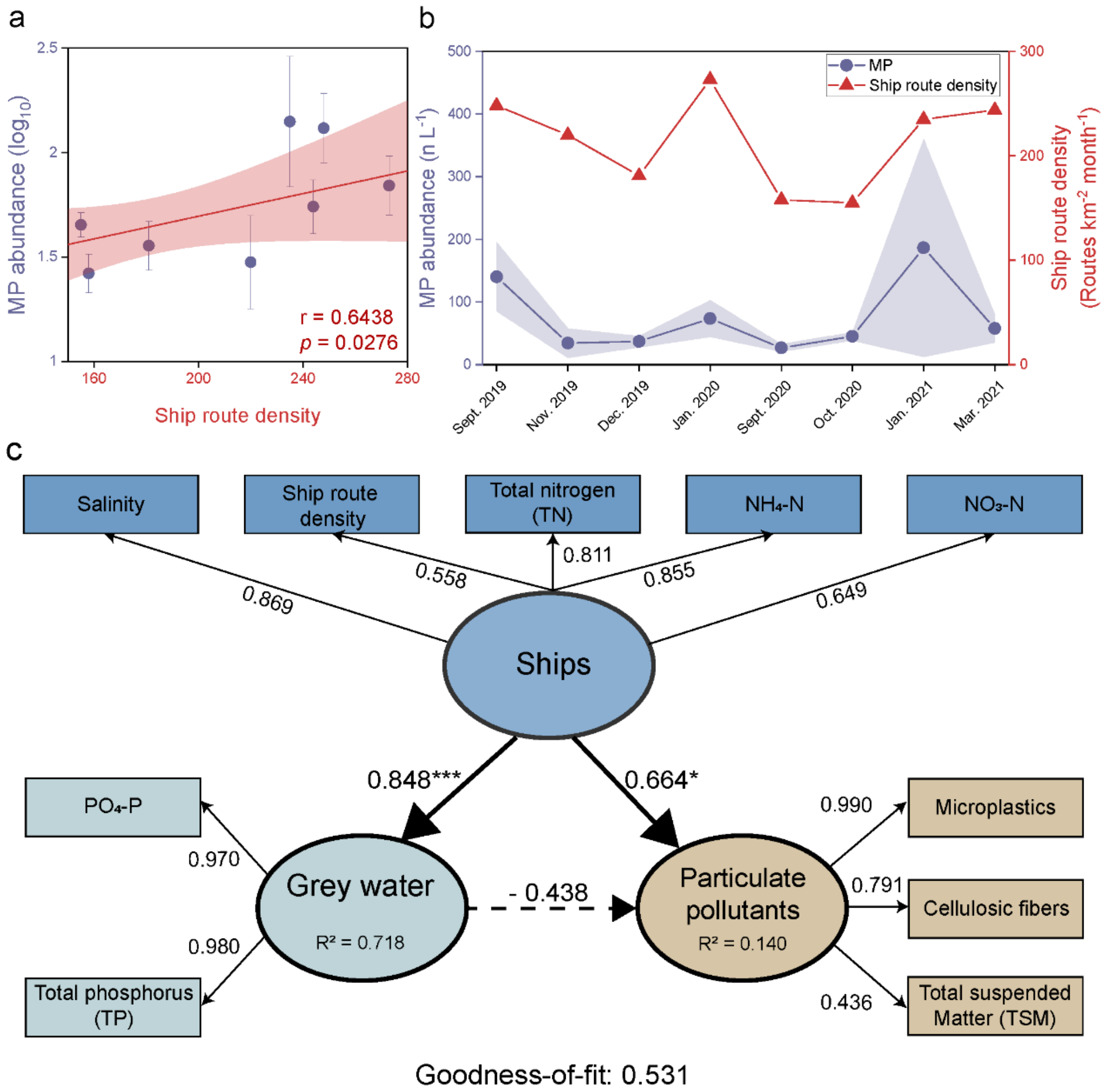

Figure 5. Positive correlations between MP abundance and ship route density (a-b), and results of the Partial Least Squares-Path Modelling (PLS-PM) on ships, nutrients and particulate pollutants (c). The inner model (ellipse) shows cause-effect relationships between ship density, graywater and particulate pollutants. The outer model (rectangles) shows ten manifest variables in reflective mode. Solid and dotted arrows in the inner model are path coefficients (positive and negative correlations) with p values indicated by asterisks (*** < 0.001, * < 0.05). Loadings of the outer model are showcased beside the arrows. Shaded area shows 95% confidence interval in (a) and standard deviation in (b). Data on monthly route density of all types of ships were obtained from European Marine Observation and Data Network (EMODnet) human activities data (www.emodnet-humanactivities.eu, last accessed 21/01/2022).

Direct effects of ships to gray water and particulate pollutants in the inner model were proven by high path coefficients. Ships greatly affects gray water (0.848, $p < 0.001$) and particulate pollutants (0.664, $p = 0.026$). There was no significant relationship between gray water and particulate pollutants, which is explained by the fact that the dataset of MVs for the two LVs was not the same type of indicators (MP and TP concentrations were measured in seawater, not in gray water). Therefore, more empirical studies are needed to prove causal relationship between gray water discharge from ships and related MP pollution. Ships also contributed to particulate pollutants indirectly (-0.371). Based on the PLS-PM, the higher pollution from TP and MP can be quantitatively and causally attributed to ships operating in the study area.

Discussion

The results from this present study during the two-year investigation before and during Covid-19 demonstrated that microfiber hotspots associated with extensive shipping and non-cargo shipping activities in a remote area. To eliminate other sources of microfibers, we noted that Brønnøysund is a city with merely 5,045 inhabitants (2018), and aquaculture derived MPs were not present based on the identification results. In addition, the EMODnet data on urban wastewater treatment (emodnet-humanactivities.eu, last accessed 20/01/2022) confirmed no direct discharge points to the coastal water from Brønnøysund (Figure S8).

Microplastics and microfibers from ships can be concentrated in gray water [46]. Our study is the first to have captured high microfiber concentration associated with waste streams from extensive shipping and non-cargo shipping activities. Although dumping of plastic waste has been banned by MARPOL Annex V, and discharge of sewage (black water) has been regulated by MARPOL Annex IV, discharge of gray water has not been regulated worldwide, and can thus be directly discharged untreated. Nevertheless, environmental impact of gray water remains largely unknown, especially as a source of unregulated pollutants, including MP and pharmaceuticals and personal care products [47, 6]. Apart from cruise ships, oil and chemical tankers, cargo ships, fishing vessels and offshore ships also discharge gray water into the ocean [7]. Regarding this issue, a more in-depth discussion on gray water from ships as significant sea-based sources of MP has been proposed [6].

Sewage and gray water released from cruise ships are a major source of marine pollution [8]. Unlike sewage, treatment of gray water from cruise ships is generally lacking before being discharged into the sea [48]. The only study to date that reported MP concentration in gray water reached up to 50,000 n L^{-1} [46], which is two orders of magnitude higher compared to our monitoring results (~500 n L^{-1}). The amount of MP discharged annually through gray water from a single cruise ship is comparable to that from a wastewater treatment plant [46]. A preliminary estimation further implies that MP discharged from gray water worldwide is at the similar magnitude of secondary MP fragmented each year at 100 thousand tons [6].

Apart from a review by the International Maritime Organization (IMO) that included gray water and sewage from ships into sources of marine litter [49], no inclusion of this source has been attempted in published papers or reports summarizing sources of MP in the environment [4, 50, 51]. However, considering the similarity of MP characteristics in the present study to a global surface water investigation in six ocean basins [2], sea-based sources of fibrous MP is largely overlooked, especially the proportion from gray water discharge. Another investigation on MP across east and west Arctic Ocean found pervasive polyester and cellulosic fibers, but suggested those fibers may be derived from domestic wastewater [52]. However, these studies did not investigate water chemistry in addition to MP investigation nor apply multivariate analysis to apportion sources. Our monitoring results unraveled that shipping and non-cargo shipping activities as major sources of MP can be extrapolated to widespread distribution of MP in the world's oceans [6]. Apart from MP fibers, the identification of the alkyd ship paint revealed that marine coatings and ship paints are also contributing to MP pollution. In the southern coast of Korea, paint particles at the coastal surface water were 12 times more than plastic fragments and fibers as a result of extensive fishing boats [44]. These findings add to new concern about pollution from ships.

The discovery of MP hotspots in the waters off a remote port city of Norway revealed a need for treatment of MP onboard ships and more robust regulations on gray water to prevent marine pollution. The Norwegian Maritime Authority (NMA) prohibited gray water discharge from ships over 2500 tonnage in Norwegian World Heritage fjords in 2019 [53]. The Norwegian coast is one of the most popular cruise destinations because of the World Heritage fjords, and sustainable tourism requires leveraging management and economic tools to avoid pollution to the environment. The caveat of the present study is that due to ongoing Covid-19 situation, we were unable to directly collect or analyze gray water samples from ships after trying all attempts. Therefore, a systematic understanding of MP in gray water and its contribution to global MP distribution is urgently required in the UN Decade of Ocean Science.

Conclusions

In this study, we monitored microplastic and microfiber variation in the waters off a remote port city of Norway before and during Covid-19, and revealed the sources of such high concentration in association with shipping and non-cargo shipping activities from gray water discharge. Considering the similarity of MP characteristics in the present study to that in the global ocean, sea-based sources of MP are largely overlooked. Regulations on gray water discharge are still lacking worldwide due to limited empirical data and understanding on its environmental impacts, especially for emerging pollutants. Microplastic pollution from sea-based sources require more systematic research in the Decade of Ocean Science.

ASSOCIATED CONTENT

Supporting Information

Map and photo of the sampling site; schematic of the portable sampling device; methods for sampling, pre-treatment, FTIR analysis, QA/QC measures; results on MP size distribution; characteristics of MP during Covid-19; Spearman's correlation between MP and environmental parameters; ship route density before and during Covid-19 and passenger ships association with MP and TN, TP; results on PLS-PM; aquaculture and wastewater discharge locations in the study area.

AUTHOR INFORMATION

Author Contributions

G.P. and C.M. conceptualized the study. G.P. analysed microplastic samples, performed formal analysis and drafted the manuscript. C.M. collected samples, acquired and analyzed data. C. J. analysed data and wrote the manuscript. B.X, X.Z. Y. S. and F. Z. interpreted data and wrote the manuscript. D.L. interpreted data, significantly revised and improved the manuscript. All authors have given approval to the final version of the manuscript.

Data availability

The authors declare that the data of this study are available from the corresponding authors upon request.

ACKNOWLEDGEMENTS

This study was funded by the China Scholarship Council (CSC: 201806140234) China Postdoctoral Science Fund (2021M690209) to Dr. Guyu Peng, and the National Natural Science Foundation of China (grant 41676190 and 51721006). B.X. thanks the China Scholarship Council and Deutscher Akademischer Austauschdienst (CSC-DAAD) for a postdoctoral scholarship.

References:

(1) UNEP. Proceedings of the United Nations Environment Assembly of the United Nations Environment Programme at its first session. **2014**, *UNEP/EA.1/10*.

(2) Suaria, G.; Achtypi, A.; Perold, V.; Lee, J.R.; Ryan, P.G. Microfibers in oceanic surface waters: A global characterization. *Science Advances*. **2020**, *6*(23), y8493.

(3) Kershaw, P.J.; Rochman, C.M. Sources, fate and effects of microplastics in the marine environment: part 2 of a global assessment. *Reports and Studies-IMO/FAO/Unesco-IOC/WMO/IAEA/UN/UNEP Joint Group of Experts on the Scientific Aspects of Marine Environmental Protection (GESAMP) Eng No. 93*. **2015**.

(4) Mitrano, D.M.; Wohlleben, W. Microplastic regulation should be more precise to incentivize both innovation and environmental safety. *Nat. Commun.* **2020**, *11*(1).

(5) Iyare, P.U.; Ouki, S.K.; Bond, T. Microplastics removal in wastewater treatment plants: a critical review. *Environmental Science: Water Research & Technology*. **2020**, *6*(10), 2664-2675.

(6) Peng, G.; Xu, B.; Li, D. Gray Water from Ships: A Significant Sea-Based Source of Microplastics? *Environ. Sci. Technol.* **2022**, *56*(1), 4-7.

(7) Ytreberg, E.; Eriksson, M.; Maljutenko, I.; Jalkanen, J.; Johansson, L.; Hassellöv, I.; Granhag, L. Environmental impacts of grey water discharge from ships in the Baltic Sea. *Mar. Pollut. Bull.* **2020**, *152*, 110891.

(8) USEPA. Cruise Ship Discharge Assessment Report. EPA842-R-07-005. **2008**.

(9) MacLeod, M.; Arp, H.P.H.; Tekman, M.B.; Jahnke, A. The global threat from plastic pollution. *Science*. **2021**, *373*(6550), 61-65.

(10) Xue, B.; Zhang, L.; Li, R.; Wang, Y.; Guo, J.; Yu, K.; Wang, S. Underestimated Microplastic Pollution Derived from Fishery Activities and "Hidden" in Deep Sediment. *Environ. Sci. Technol.* **2020**, *54*(4), 2210-2217.

(11) Galgani, F.; Hanke, G.; Maes, T. in *Marine Anthropogenic Litter*, eds. Bergmann M., Gutow L. and Klages M., Cham, Springer International Publishing, 2015, pp. 29-56.

(12) Oliveira, A.R.; Sardinha-Silva, A.; Andrews, P.L.R.; Green, D.; Cooke, G.M.; Hall, S.; Blackburn, K.; Sykes, A.V. Microplastics presence in cultured and wild-caught cuttlefish, Sepia officinalis. *Mar. Pollut. Bull.* **2020**, *160*, 111553.

(13) Rummel, C.D.; Jahnke, A.; Gorokhova, E.; Kühnel, D.; Schmitt-Jansen, M. Impacts of Biofilm Formation on the Fate and Potential Effects of Microplastic in the Aquatic Environment. *Environmental Science & Technology Letters*. **2017**, *4*(7), 258-267.

(14) Vethaak, A.D.; Legler, J. Microplastics and human health. *Science*. **2021**, *371*.

(15) Golmen, L.G.; Eikrem, W.; Staalstrøm, A.; Mengeot, C.; Frigstad, H. ØKOKYST–DP Norskehavet Sør (II). Årsrapport 2019. *NIVA-rapport*. **2020**.

(16) Isobe, A.; Buenaventura, N.T.; Chastain, S.; Chavanich, S.; Cózar, A.; DeLorenzo, M.; Hagmann, P.; Hinata, H.; Kozlovskii, N.; Lusher, A.L.; Martí, E.; Michida, Y.; Mu, J.; Ohno, M.; Potter, G.; Ross, P.S.; Sagawa, N.; Shim, W.J.; Song, Y.K.; Takada, H.; Tokai, T.; Torii, T.; Uchida, K.; Vassillenko, K.; Viyakarn, V.; Zhang, W. An interlaboratory comparison exercise for the determination of microplastics in standard sample bottles. *Mar. Pollut. Bull.* **2019**, *146*, 831-837.

(17) Koelmans, A.A.; Mohamed Nor, N.H.; Hermsen, E.; Kooi, M.; Mintenig, S.M.; De France, J. Microplastics in freshwaters and drinking water: Critical review and assessment of data quality. *Water Res.* **2019**, *155*, 410-422.

(18) Merga, L.B.; Redondo-Hasselerharm, P.E.; Van den Brink, P.J.; Koelmans, A.A. Distribution of microplastic and small macroplastic particles across four fish species and sediment in an African lake. *Sci. Total Environ.* **2020**, *741*, 140527.

(19) Kooi, M.; Koelmans, A.A. Simplifying Microplastic via Continuous Probability Distributions for Size, Shape, and Density. *Environmental Science & Technology Letters*. **2019**, *6*(9), 551-557.

(20) Sanchez, G. PLS path modeling with R. *Berkeley: Trowchez Editions*. **2013**, *383*, 2013.

(21) Uurasjärvi, E.; Pääkkönen, M.; Setälä, O.; Koistinen, A.; Lehtiniemi, M. Microplastics accumulate to thin layers in the stratified Baltic Sea. *Environ. Pollut.* **2021**, *268*, 115700.

(22) Zhou, Q.; Tu, C.; Yang, J.; Fu, C.; Li, Y.; Waniek, J.J. Trapping of microplastics in halocline and turbidity layers of the semi-enclosed Baltic Sea. *Frontiers in Marine Science*. **2021**, 1555.

(23) Redfield, A.C. The biological control of chemical factors in the environment. *Science progress*. **1960**, *11*, 150-170.

(24) Neill, M. A method to determine which nutrient is limiting for plant growth in estuarine waters—at any salinity. *Mar. Pollut. Bull.* **2005**, *50*(9), 945-955.

(25) Sun, J.; Dai, X.; Wang, Q.; van Loosdrecht, M.C.M.; Ni, B. Microplastics in wastewater treatment plants: Detection, occurrence and removal. *Water Res.* **2019**, *152*, 21-37.

(26) Zhu, J.; Zhang, Q.; Li, Y.; Tan, S.; Kang, Z.; Yu, X.; Lan, W.; Cai, L.; Wang, J.; Shi, H. Microplastic pollution in the Maowei Sea, a typical mariculture bay of China. *Sci. Total Environ.* **2019**, *658*, 62-68.

(27) Yan, M.; Nie, H.; Xu, K.; He, Y.; Hu, Y.; Huang, Y.; Wang, J. Microplastic abundance, distribution and composition in the Pearl River along Guangzhou city and Pearl River estuary, China. *Chemosphere*. **2019**, *217*, 879-886.

(28) Qu, X.; Su, L.; Li, H.; Liang, M.; Shi, H. Assessing the relationship between the abundance and properties of microplastics in water and in mussels. *Sci. Total Environ.* **2018**, *621*, 679-686.

(29) Jang, M.; Shim, W.J.; Cho, Y.; Han, G.M.; Song, Y.K.; Hong, S.H. A close relationship between microplastic contamination and coastal area use pattern. *Water Res.* **2020**, *171*, 115400.

(30) Desforges, J.W.; Galbraith, M.; Dangerfield, N.; Ross, P.S. Widespread distribution of microplastics in subsurface seawater in the NE Pacific Ocean. *Mar. Pollut. Bull.* **2014**, *79*(1-2), 94-99.

(31) Zhao, S.; Zhu, L.; Li, D. Microplastic in three urban estuaries, China. *Environ. Pollut.* **2015**, *206*, 597-604.

(32) Cai, M.; He, H.; Liu, M.; Li, S.; Tang, G.; Wang, W.; Huang, P.; Wei, G.; Lin, Y.; Chen, B.; Hu, J.; Cen, Z. Lost but can't be neglected: Huge quantities of small microplastics hide in the South China Sea. *Sci. Total Environ.* **2018**, *633*, 1206-1216.

(33) Enders, K.; Lenz, R.; Stedmon, C.A.; Nielsen, T.G. Abundance, size and polymer composition of marine microplastics ≥10μm in the Atlantic Ocean and their modelled vertical distribution. *Mar. Pollut. Bull.* **2015**, *100*(1), 70-81.

(34) Xu, P.; Peng, G.; Su, L.; Gao, Y.; Gao, L.; Li, D. Microplastic risk assessment in surface waters: A case study in the Changjiang Estuary, China. *Mar. Pollut. Bull.* **2018**, *133*, 647-654.

(35) Zhao, S.; Wang, T.; Zhu, L.; Xu, P.; Wang, X.; Gao, L.; Li, D. Analysis of suspended microplastics in the Changjiang Estuary: Implications for riverine plastic load to the ocean. *Water Res.* **2019**, *161*, 560-569.

(36) Lusher, A.L.; Tirelli, V.; O Connor, I.; Officer, R. Microplastics in Arctic polar waters: the first reported values of particles in surface and sub-surface samples. *Sci. Rep.-Uk*. **2015**, *5*, 14947.

(37) Sun, X.; Liu, T.; Zhu, M.; Liang, J.; Zhao, Y.; Zhang, B. Retention and characteristics of

microplastics in natural zooplankton taxa from the East China Sea. *Sci. Total Environ.* **2018**, *640-641*, 232-242.
(38) Kwon, O.Y.; Kang, J.; Hong, S.H.; Shim, W.J. Spatial distribution of microplastic in the surface waters along the coast of Korea. *Mar. Pollut. Bull.* **2020**, *155*, 110729.
(39) Sadri, S.S.; Thompson, R.C. On the quantity and composition of floating plastic debris entering and leaving the Tamar Estuary, Southwest England. *Mar. Pollut. Bull.* **2014**, *81*(1), 55-60.
(40) Zhang, W.; Zhang, S.; Wang, J.; Wang, Y.; Mu, J.; Wang, P.; Lin, X.; Ma, D. Microplastic pollution in the surface waters of the Bohai Sea, China. *Environ. Pollut.* **2017**, *231*, 541-548.
(41) Beer, S.; Garm, A.; Huwer, B.; Dierking, J.; Nielsen, T.G. No increase in marine microplastic concentration over the last three decades – A case study from the Baltic Sea. *Sci. Total Environ.* **2018**, *621*, 1272-1279.
(42) Isobe, A.; Uchiyama-Matsumoto, K.; Uchida, K.; Tokai, T. Microplastics in the Southern Ocean. *Mar. Pollut. Bull.* **2017**, *114*(1), 623-626.
(43) He, X.; Wang, J.; Zhao, B.; Mu, Y.; Liu, Y.; Hou, W.; Ma, T. NonDestructive Discrimination of Ship Deck Paint Using Attenuated Total Reflection - Fourier Transform Infrared (ATR-FTIR) Spectroscopy with Chemometric Analysis. *Anal. Lett.* **2020**, *53*(17), 2761-2774.
(44) Song, Y.K.; Hong, S.H.; Jang, M.; Kang, J.; Kwon, O.Y.; Han, G.M.; Shim, W.J. Large Accumulation of Micro-sized Synthetic Polymer Particles in the Sea Surface Microlayer. *Environ. Sci. Technol.* **2014**, *48*(16), 9014-9021.
(45) Lee, H.; Lee, D.; Seo, J.M. Analysis of paint traces to determine the ship responsible for a collision. *Sci. Rep.-Uk*. **2021**, *11*(1).
(46) Mikkola, O. Estimating microplastic concentrations and loads in cruise ship grey waters. Master's thesis. Aalto University. **2020**.
(47) Svavarsson, J.; Guls, H.D.; Sham, R.C.; Leung, K.M.Y.; Halldórsson, H.P. Pollutants from shipping - new environmental challenges in the subarctic and the Arctic Ocean. *Mar. Pollut. Bull.* **2021**, *164*, 112004.
(48) Klein, R.A. Responsible Cruise Tourism: Issues of Cruise Tourism and Sustainability. *Journal of Hospitality and Tourism Management*. **2011**, *18*(1), 107-116.
(49) IMO. Progress report of the GESAMP Working Group on Sea-based Sources of Marine Litter Note by the Secretariat. MEPC 75/8. **2020**.
(50) Law, K.L.; Narayan, R. Reducing environmental plastic pollution by designing polymer materials for managed end-of-life. *Nature reviews. Materials*. **2021**.
(51) Galafassi, S.; Nizzetto, L.; Volta, P. Plastic sources: A survey across scientific and grey literature for their inventory and relative contribution to microplastics pollution in natural environments, with an emphasis on surface water. *Sci. Total Environ.* **2019**, *693*, 133499.
(52) Ross, P.S.; Chastain, S.; Vassilenko, E.; Etemadifar, A.; Zimmermann, S.; Quesnel, S.; Eert, J.; Solomon, E.; Patankar, S.; Posacka, A.M.; Williams, B. Pervasive distribution of polyester fibres in the Arctic Ocean is driven by Atlantic inputs. *Nat. Commun.* **2021**, *12*(1), 106.
(53) NMA, Amendments to the regulations on environmental safety for ships and mobile offshore units. **2019**.